

First-principles study of wurtzite InN (0001) and (000 $\bar{1}$) surfacesChee Kwan Gan¹ and David J. Srolovitz²¹Institute of High Performance Computing, 1 Science Park Road, Singapore 117528, Singapore²Department of Physics, Yeshiva University, New York, NY 10033, USA

(Dated: May 19, 2006)

Density-functional calculations are used to study various plausible structures of the wurtzite InN (0001) and (000 $\bar{1}$) surfaces. These structures include the unreconstructed surfaces, surfaces with m monolayers of In or N, several possible coverages and locations of In or N adatoms and vacancies. The stable structure of the (0001) surface under N-rich conditions is the unreconstructed, In-terminated surface, while under In-rich conditions the stable surface has a 3×4 monolayer of In atoms. The stable structure of the InN (000 $\bar{1}$) surface corresponds to a full monolayer of In atoms in the atop sites (directly above the N atoms) over the entire range of accessible In (or N) chemical potential. The atomic structures of the low-energy structures are also discussed.

PACS numbers: 68.47.Fg

Keywords: InN surfaces, surface reconstruction, group-III nitrides

I. INTRODUCTION

Group-III nitrides are of considerable interest for applications in laser and light-emitting diodes^{1,2,3}. Alloying different group-III elements in nitride compounds (e.g., $\text{Al}_x\text{Ga}_{1-x}\text{N}$ or $\text{In}_x\text{Ga}_{1-x}\text{N}$) provides a means of tuning the band gap over a wide spectral range (e.g., from blue to infrared in the case of $\text{In}_x\text{Ga}_{1-x}\text{N}$). The growth of high quality group-III nitride compounds can be a considerable challenge and a barrier to the successful transition of these materials into applications. The connection between vapor phase growth processes and

film quality can usually be traced back to the interplay of growth conditions and surface structure. While there have been several theoretical studies on the surfaces of group-III nitrides, these have largely focused upon AlN and GaN^{4,5,6,7,8,9,10,11}. Relatively little theoretical analysis has been devoted to the surfaces of InN, largely because the level of interest in this material has been limited by difficulty in producing this material.

InN is an attractive material for electronic and optoelectronic applications because it possesses a series of outstanding properties¹², such as a small effective mass¹³ (leading to a large electron mobility and a high carrier saturation velocity). The steady-state drift velocity in InN is 4.2×10^7 cm/s is significantly larger than that of many III-V competitors, GaN (2.9×10^7 cm/s), AlN (1.7×10^7 cm/s), and GaAs (1.6×10^7 cm/s)^{12,14}. Since InN exhibits a high peak overshoot velocity¹⁴, it is a good candidate for high-performance heterojunction field-effect transistors.

The growth of high quality InN is difficult compared to other III-nitrides, such as AlN and GaN, because it has a relatively low dissociation temperature and a high equilibrium N_2 vapor pressure^{15,16}. The lack of suitable substrate materials also hinders the use of InN as a heteroepitaxial thin film. Nonetheless, several groups^{17,18,19} have successfully grown good quality InN single crystals. Interestingly, they have reported bandgaps of approximately 0.9 eV, which is quite small compared to the com-

mon only accepted values of 1.8 eV to 2.1 eV.

Since InN does not possess a center of symmetry, the (0001) and (000 $\bar{1}$) surfaces are different. The first is In-terminated, while the latter is N-terminated. Experimental evidence suggests that polarity (termination) is an important consideration in the growth of high quality group-III nitride semiconductors²⁰. For example, surface with opposite polarity exhibit different morphologies²¹. Radio frequency molecular beam epitaxial (rf-MBE) growth of InN on sapphire²⁰ produces different polarity surfaces depending on growth temperature (N-terminated at low temperature, In-terminated at high temperature). This demonstrates that growth conditions can modify the relative growth rates of surfaces with opposite polarity. The observed change in the relative growth rates of surfaces with opposite polarity with temperature may be associated with different activation energies for growth or may be indicative a change in surface structure with growth conditions. In this work, we determine the equilibrium structure of the important (0001) and (000 $\bar{1}$) surfaces of InN as a function of growth conditions. In particular, we examine the role of In (or N) chemical potential on the equilibrium surface structure. We vary chemical potential rather than temperature, since the range of chemical potentials that are experimentally accessible is much larger than that for temperature in the most common group-III nitride growth methods (i.e., MOCVD).

II. THEORETICAL MODELS

The present calculations are performed within the local density approximation (LDA) framework, as implemented within the Vienna Simulation Package (VASP)²², employing ultrasoft pseudopotentials²³. The important²⁴ 4d states for In are included as valence electrons in the pseudopotentials. Throughout this work, we employed a relatively high cutoff energy of 435 eV. We first optimize the bulk wurtzite InN structure, yielding the following

lattice parameters²⁵: $a = 3.518 \text{ \AA}$, $c = 5.690 \text{ \AA}$, and the internal parameter $u = 0.379$. These lattice parameters are in very good agreement with those found from experiment¹⁷; $a = 3.5365 \text{ \AA}$ and $c = 5.7039 \text{ \AA}$.

For the surface calculations, our supercells contained six (0001) bilayers in which the lower four bilayers were fixed in the bulk configuration. The upper two bilayers and any adatoms or adlayers were allowed to relax. Our system is larger than those used by many others in studies of other group-III nitride surfaces, where typically four bilayers^{6,7,9,10} were employed. To prevent unphysical charge transfer between the top and bottom slab surfaces, pseudo-hydrogens with fractional charges are used. For the In-terminated (0001) surface, the dangling bonds in the N layer are saturated with pseudo-hydrogens with a fractional charge of $3/4$. For the N-terminated (000 $\bar{1}$) surface, we saturate the dangling bonds in the In layer with pseudo-hydrogens with a fractional charge of $5/4$. We employ a $2 \times 2 \times 1$ Monkhorst-Pack set sampling scheme for the surface supercell, which gives two irreducible k -points. The structural optimizations were terminated when the magnitude of the Hellmann-Feynman force on each ion is less than 1 m Ry/Bohr (25.7 meV/\AA). We perform calculations with vacuum thicknesses of both 12.9 \AA and 15.7 \AA . These two sets of calculations yield almost identical results, showing the appropriateness of the vacuum thickness employed. Hereafter we present the results obtained with a vacuum thickness of 15.7 \AA .

We consider various vacancy, adatom, trimer, and monolayer surface structures that satisfy the electron counting rule⁵. It is useful to refer to Fig. 1 (a), which shows two (0001) layers of atoms in a 2×2 surface unit cell, in order to understand the structures. The surfaces considered include a perfect surface [as shown by the black circles in Fig. 1 (a)], a monolayer of In (or N) atoms directly above each In (or N) terminating atom [i.e., this is 4 atop atoms in the 2×2 cell of Fig. 1 (a)], a quarter-monolayer of adatoms with the adatoms directly atop one of the In (or N) atoms (T4 sites) in the 2×2 cell, a quarter-monolayer of adatoms with the adatoms centered between three surface atoms (H3 sites), a single vacancy in the terminating plane of the 2×2 cell, and a triangle of three In (or N) atoms on H3 or T4 sites (i.e., a trimer). The relaxed structure of a representative case of an In trimer on the T4 sites is shown in Figs. 1 (b) and 1 (c).

The relative formation energies of the different surfaces are calculated within the thermodynamically allowed range of the In chemical potential μ_{In} . The chemical potentials of In and N are related through²⁶

$$\mu_{\text{In}} + \mu_{\text{N}} = \mu_{\text{InN (bulk)}} : \quad (1)$$

Operationally, we can define the chemical potential $\mu_{\text{In (bulk)}}$ as the total energy per cation-anion pair $E(\text{InN}_{\text{bulk}})$ in wurtzite InN at 0 K . The chemical potential of In is bounded above by that of the pure, tetragonal In metal²⁷, denoted by $\mu_{\text{In}}^0 = E(\text{In})$. Similarly, the chemical potential of N is bounded above by that of a nitrogen

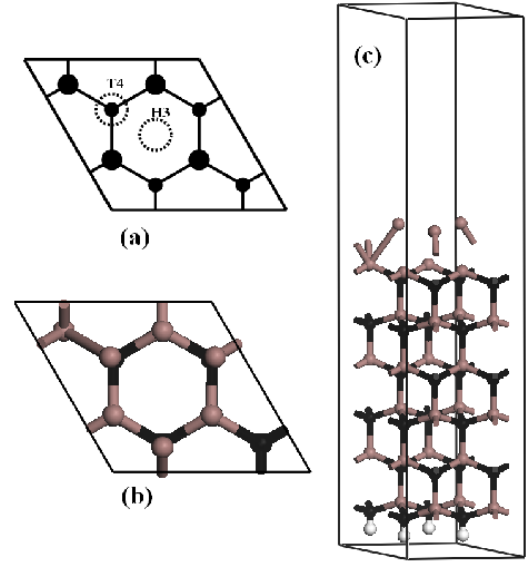


FIG. 1: (Color online) (a) A schematic of the atom positions in the top two atomic planes of a 2×2 unit cell of the f0001g surface. The larger and smaller filled circles denote indium atoms on the surface and nitrogen atoms one plane down, respectively, for the In-terminated (0001) surface. The same schematic describes the (000 $\bar{1}$) surface, but with the elemental identity of the atoms switched. The locations of the H3 (hollow) and T4 (top) sites are labeled by dotted circles. (b) A view of an In trimer residing on the T4 sites from above. The gray and black atoms denote the In and N atoms, respectively. Notice that a nitrogen atom is exposed in the lower right corner of the image. (c) The side view of the 2×2 unit cell. Four pseudo-hydrogen atoms (shown in white) are found at the bottom of the cell.

molecule N_2 , denoted by $\mu_{\text{N}}^0 = \frac{1}{2}E(\text{N}_2)$. The enthalpy of formation of InN is simply

$$H = \mu_{\text{InN (bulk)}} - \mu_{\text{N}}^0 - \mu_{\text{In}}^0 \quad (2)$$

where $E(\text{In})$, $E(\text{N}_2)$, and $E(\text{InN}_{\text{bulk}})$ are determined from total energy calculations within LDA. The calculated enthalpy of formation of InN, $H = -0.376 \text{ eV}$, agrees reasonably well with the experimental value^{28,29} of -0.28 eV . The fact that these calculations suggest that InN is more strongly bound than in experiments is not surprising since the LDA tends to lead to overbinding. The small enthalpy of formation implies that InN has a low thermal stability compared with other group-III nitrides such as GaN and AlN where the experimental formation enthalpies^{28,29} are -1.23 eV (i.e., 4 times larger than for InN) and -3.21 eV (i.e., 11 times larger than for InN), respectively.

The formation energy of any structure is calculated from

$$\begin{aligned} E_{\text{form}} &= E_{\text{opt}} - n_{\text{In}} \mu_{\text{In}} - n_{\text{N}} \mu_{\text{N}} \\ &= E_{\text{opt}} - n_{\text{In}} (\mu_{\text{In}} - \mu_{\text{In}}^0) - n_{\text{N}} (\mu_{\text{N}} - \mu_{\text{N}}^0) - n_{\text{In}} \mu_{\text{In}}^0 - n_{\text{N}} \mu_{\text{N}}^0 ; \quad (3) \end{aligned}$$

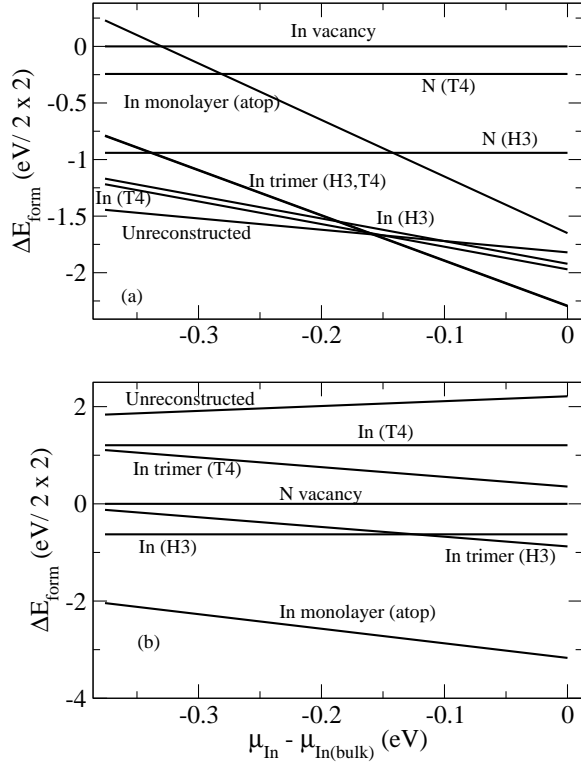


FIG. 2: The relative formation energies for the 2×2 unit cell of Fig. 1(a) as a function of the In chemical potential for the (a) (0001) and (b) (000 $\bar{1}$) surfaces. The formation energies are all referenced to that of the surface with a single vacancy on the surface atomic plane.

where E_{opt} is the total energy of the structure resulting from the optimization of the structure with respect to atomic positions and n_{In} and n_{N} are the number of In and N atoms in the structure, respectively. We have used Eq. (1) to eliminate n_{N} to arrive at the second line of Eq. (3). Equations (1) and (2) show that the thermodynamically allowed range of the chemical potential of In is $\mu_{\text{H}} + \frac{0}{\text{In}} \leq \mu_{\text{In}} \leq \frac{0}{\text{In}}$.

III. THE (0001) SURFACE

The relative formation energies for the 2×2 InN (0001) unit cell of Fig. 1(a) are shown in Fig. 2(a) for the surface structures described above as a function of the In chemical potential. In this figure, we reference the energy to that of the 2×2 InN (0001) unit cell with a single In vacancy in the surface atomic plane. This simplifies the comparison of energies between the different structures, as well as leads to the cancellation of the contribution to E_{opt} in Eq. (3) from the chemical potential of pseudo-hydrogen atoms. We omit the curves for the structures of energies greater than 0.25 eV. Note that the slopes of the lines in Fig. 2 simply follow from the fact that the different structures have different numbers of In and N atoms (see Eq. (3)).

The surface with an N adatom on the H3 site has a lower energy than that with an N adatom on the T4 site by 0.70 eV/2. This is largely due to a stronger electrostatic repulsion between the T4 nitrogen adatom and the nitrogen atom below. Similar behavior has been observed for the AlN⁵ (0001) and GaN⁷ (0001) surfaces. The surface with an In adatom on the T4 site has a lower energy than that with an In adatom on the H3 site since there is an electrostatic attraction between the In adatom on the T4 site and the N atom below. The surface with a full In monolayer with atoms on the atop sites has a relatively high energy compared with the other (0001) surfaces.

Under N-rich conditions (low In chemical potential), the bare 1×1 (In terminated) surface [as shown in Fig. 1(a)] has the lowest energy. Our calculations also show that surfaces in which the In trimer resides on either the T4 or H3 sites yield essentially the same energy, despite the fact that In atoms are directly above N atoms in the T4 In trimer model. Similar behavior is observed for the AlN (000 $\bar{1}$)⁵ surface where Al trimers on the T4 or H3 sites have the same energy. This shows that arguments based solely on electrostatic interactions are not sufficient to explain even the qualitative behavior of many of the adatom reconstructed surfaces. Figure 2(a) shows that under In-rich (large In chemical potential) conditions, the stable (0001) surface have In trimers, located on either T4 or H3 sites. The present results for the stable (0001) InN surface are significantly different than the same surface in other group-III nitrides across the entire range of chemical potentials. For AlN (0001)⁵ and GaN (0001)⁷ surfaces, the surface with an N adatom on the H3 site is found to be energetically favorable under N-rich conditions, while the surface structure with a metal atom (i.e., Al or Ga) on the T4 site is energetically favorable under metal-rich conditions.

Examination of the unreconstructed InN (0001) surface [as shown in Fig. 1(a)] shows that the In-N bilayer spacings for the first and second bilayers are 0.654 Å and 0.655 Å, respectively. These are slightly smaller than the ideal, bulk spacing of 0.688 Å. The spacing between In-In atomic planes are 2.862 Å and 2.825 Å for the first and second pairs, as compared with a bulk spacing of 2.845 Å. This shows that the spacing between the first In-In layer expands, while the second contracts, relative to the bulk spacing. Similar oscillatory surface relaxations are observed in other systems (e.g., see Ref. 30).

For the InN (0001) surface with a single In vacancy on the surface layer, we find that the top-layer In atoms undergo sp^2 bonding configuration by relaxing vertically. This reduces the bond length between the threefold-coordinated In and the threefold-coordinated N atoms from the ideal value of 2.145 Å to 2.050 Å. This 4.4 % reduction in length is comparable to that for the case of AlN⁵, where a 6% contraction in the distance between the Al and N atoms in the vacancy model of AlN (0001) surface was observed. The vertical movement of the top layer atoms reduces the top In-N bilayer spacing from the

ideal value of 0.688 Å to 0.350 Å.

The surface with an In trimer on the T4 or H3 sites have the same energy and are the most stable surfaces at large In chemical potential, as discussed above. It is interesting to note that the interlayer spacing between the trimer In atoms and the In atoms in the next plane are 2.61 Å for the T4 site trimer and 2.60 Å for the H3 site trimer. Hence, these two surface configurations are very similar both structurally and energetically.

IV. THE (000 $\bar{1}$) SURFACE

The relative formation energies for the 2 × 2 InN (000 $\bar{1}$) unit cell of Fig. 1 (a) are shown in Fig. 2 (b) for the surface structures described above as a function of the In chemical potential. In this figure, we reference the energy to that of the 2 × 2 InN (000 $\bar{1}$) unit cell with a single N vacancy in the surface atomic plane. No results are presented for the surfaces with N adatom or N trimers since these systems are unstable. Northrup et al.⁵ argued that the relatively small size of the N atom makes surfaces with N adatoms or trimers on the AlN (000 $\bar{1}$) highly unstable. It is therefore not surprising that our calculations also show that N trimer or N adatom models are not stable since the single-bond covalent radius³¹ of In (1.48 Å) is considerable larger than that of Al (1.30 Å).

The relaxed unreconstructed InN (000 $\bar{1}$) surface (N-terminated) has a very large formation energy, relative to most of the other surface structures. We find that the surfaces with an In adatom on the H3 site has an energy that is 1.83 eV / (2 × 2) lower than that with the In adatom on the T4 site. This may be attributed to the fact that there is greater electrostatic repulsion between the T4 In adatom and the In atom directly below it than between the H3 In adatom and the more distant In atoms two atomic planes below. Similar argument also holds for In trimer models, where the H3 In trimer has a lower in energy than the T4 In trimer by 1.23 eV / (2 × 2). The surface with an In monolayer with the atoms on the atop sites has the lowest energy across the entire allowed range of In chemical potential. The next lowest energy structure under N-rich (low In chemical potential) conditions is surface with a single In adatom in the 2 × 2 unit cell on the H3 site. These results contrast with the results for other group-III nitrides (000 $\bar{1}$) surfaces. In AlN and GaN, the lowest energy surface structure corresponds to an Al monolayer (atop sites occupied)⁵ or Ga monolayer³² only under metal-rich conditions. However, under N-rich conditions, the (000 $\bar{1}$) surfaces with a single Al or Ga atom on the H3 site in the 2 × 2 unit cell have the lowest energy.

Examination of the InN (000 $\bar{1}$) surface with an In monolayer with the In atoms on the atop sites is the lowest energy structure over the entire chemical potential range, as mentioned above. The In-N bilayer spacing for the top two bilayers are 0.519 Å and 0.510 Å, as compared with a bulk spacing of 0.668 Å. The In-In atomic

plane separations are 2.482 Å, 2.423 Å, and 2.593 Å for the first three pairs (counted from the surface), as compared with the bulk value of 2.845 Å. This is a substantial contraction that oscillates as it decays slowly into the bulk.

The surface structure corresponding to an In adatom in the H3 site also has a relatively low energy. This adatom is situated 0.808 Å above the triangle of three N atoms in the plane below. The corresponding In-N bond length is 1.980 Å. The three N atoms that form this triangle (i.e., nearest neighbors of the In H3 adatom) are displaced upward, toward the In adatom by 0.424 Å relative to the other, threefold-coordinated surface N atoms.

In the InN (000 $\bar{1}$) surface structure with a single N-vacancy in the 2 × 2 unit cell, the top-layer N atoms undergo substantial vertical relaxation. In this structure, the N-In bilayer spacing is 0.328 Å as compared with the bulk spacing of 0.688 Å. The bond length between the threefold-coordinated N and In atoms is also reduced from the ideal value of 2.145 Å to 1.898 Å. This is an 11.5% reduction in bond length, which is much larger than the 6% contraction observed in the N vacancy surface structure of AlN (000 $\bar{1}$)⁵. This large contraction may be attributed to the system trying to move toward a configuration that is sp² bonded.

V. CONCLUSIONS

We have performed density-functional calculations to determine the stable structure of both the InN (0001) and (000 $\bar{1}$) surfaces as a function of the In (or N) chemical potential. We considered twelve plausible surface structures. Several earlier studies considered the structure of this surface in other group-III nitrides. While structurally similar, InN is quite distinct, as indicated by a much lower heat of formation than the others (BN, AlN, GaN).

For the (0001) surface, we find that the relaxed, unreconstructed InN (0001) (In terminated) surface is stable under N-rich (low In chemical potential) conditions. On the other hand, under In rich (large In chemical potential) conditions, the stable structure corresponds to a trimer of In adatoms on either H3 or T4 sites (this is 3=4 of an In monolayer). These stable (0001) surface structures differ from those found for two other closely related group-III nitrides over the entire range of accessible chemical potentials. The stable structure of the InN (000 $\bar{1}$) surface corresponds to a monolayer of In atoms directly above the surface N atoms. This structure is stable over the entire range of accessible chemical potentials. In AlN and GaN, the same surface structure was only found to be stable under metal-rich conditions.

The present results provide guidance for the exploitation of different thin film growth methods/conditions in order to exploit the dependence of equilibrium reconstructions on chemical potential. Unlike in GaN or AlN, the stable structure of the important (0001) surface can

be manipulated by changes in growth condition.

supported by Visiting Investigator Program, Agency for Science, Technology and Research (A*STAR), Singapore.

VI. ACKNOWLEDGMENTS

The authors gratefully acknowledge useful discussions with Y. Y. Sun on surface calculations. This work was

-
- ¹ S. Nakamura, M. Senoh, S. Nagahama, N. Iwasa, T. Yamada, T. Matsushita, H. Kiyoku, and Y. Sugimoto, *Jpn. J. Appl. Phys.* **35**, Part II, L74 (1996).
 - ² S. Nakamura and G. Fasol, *The Blue Laser Diode: GaN Based Light Emitters and Lasers* (Springer, Berlin, Heidelberg, 1997).
 - ³ Y. Taniyasu, M. Kasu, and T. Makimoto, *Nature* **441**, 325 (2006).
 - ⁴ J. E. Northrup and J. Neugebauer, *Phys. Rev. B* **53**, R10477 (1996).
 - ⁵ J. E. Northrup, R. DiFelice, and J. Neugebauer, *Phys. Rev. B* **55**, 13878 (1997).
 - ⁶ A. R. Smith, R. M. Feenstra, D. W. Greve, J. Neugebauer, and J. E. Northrup, *Phys. Rev. Lett.* **79**, 3934 (1997).
 - ⁷ K. Rapcewicz, M. BuongiornoNardelli, and J. Bernholc, *Phys. Rev. B* **56**, R12725 (1997).
 - ⁸ J. Fritsch, O. F. Sankey, K. E. Schmidt, and J. B. Page, *Phys. Rev. B* **57**, 15360 (1998).
 - ⁹ F. H. Wang, P. K. Ruger, and J. Pollmann, *Phys. Rev. B* **64**, 035305 (2001).
 - ¹⁰ C. D. Lee, Y. Dong, R. M. Feenstra, J. E. Northrup, and J. Neugebauer, *Phys. Rev. B* **68**, 205317 (2003).
 - ¹¹ V. Timon, S. Brand, S. J. Clark, M. C. Gibson, and R. A. Abram, *Phys. Rev. B* **72**, 035327 (2005).
 - ¹² A. G. Bhuiyan, A. Hashimoto, and A. Yamamoto, *J. Appl. Phys.* **94**, 2779 (2003).
 - ¹³ S. N. Mohammad and H. Morkoc, *Prog. Quant. Electr.* **20**, 361 (1996).
 - ¹⁴ B. E. Foutz, S. K. O'Leary, M. S. Shur, and L. F. Eastman, *J. Appl. Phys.* **85**, 7727 (1999).
 - ¹⁵ J. B. MacChesney, P. M. Bridenbaugh, and P. B. O'Connor, *Mater. Res. Bull.* **5**, 783 (1970).
 - ¹⁶ O. Ambacher, M. S. Brandt, R. Dimitrov, T. Metzger, M. Stutzmann, R. A. Fischer, A. Meyer, A. Bergmaier, and G. Dollinger, *J. Vac. Sci. Technol. B* **14**, 3532 (1996).
 - ¹⁷ V. Y. Davydov, A. A. Kichikhin, R. P. Seisyan, V. V. Emptsev, S. V. Ivanov, F. Bechstedt, J. Furthmüller, H. Harima, A. V. Mudryi, J. Aderhold, O. Semchinova, and J. Graul, *Phys. Stat. Sol. (B)* **229**, R1 (2002).
 - ¹⁸ J. Wu, W. Walukiewicz, K. M. Yu, J. W. A. III, E. E. Haller, H. Lu, W. J. Scha, Y. Saito, and Y. Nanishi, *Appl. Phys. Lett.* **80**, 3967 (2002).
 - ¹⁹ Y. Nanishi, Y. Saito, and T. Yamaguchi, *Jpn. J. Appl. Phys.* **42**, Part I, 2549 (2003).
 - ²⁰ Y. Saito, Y. Tanabe, T. Yamaguchi, N. Teraguchi, A. Suzuki, T. Arai, and Y. Nanishi, *Phys. Stat. Sol. (B)* **228**, 13 (2001).
 - ²¹ B. Daudin, J. L. Rouviere, and M. Alery, *Appl. Phys. Lett.* **69**, 2480 (1996).
 - ²² G. Kresse and J. Furthmüller, *Phys. Rev. B* **54**, 11169 (1996).
 - ²³ D. Vanderbilt, *Phys. Rev. B* **41**, R7892 (1990).
 - ²⁴ A. F. Wright and J. S. Nelson, *Phys. Rev. B* **51**, 7866 (1995).
 - ²⁵ C. K. Gan, Y. P. Feng, and D. J. Srolovitz, *Phys. Rev. B* **73**, 235214 (2006).
 - ²⁶ G. X. Qian, R. M. Martin, and D. J. Chadi, *Phys. Rev. B* **38**, 7649 (1988).
 - ²⁷ J. Graham, A. Moore, and G. V. Raynor, *J. Inst. Metals* **84**, 86 (1956).
 - ²⁸ W. A. Harrison, *Electronic structure and the properties of solids* (Dover Publications, New York, 1989).
 - ²⁹ C. Kittel, *Introduction to Solid State Physics* (John Wiley and Sons, New York, 1996), 7th ed.
 - ³⁰ Y. Y. Sun, H. Xu, J. C. Zheng, J. Y. Zhou, Y. P. Feng, A. C. H. Huan, and A. T. S. Wee, *Phys. Rev. B* **68**, 115420 (2003).
 - ³¹ F. A. Cotton, G. Wilkinson, and P. L. Gaus, *Basic Inorganic Chemistry* (John Wiley and Sons, New York, 1995), 3rd ed.
 - ³² C. K. Gan and D. J. Srolovitz (2006), unpublished.